Inorg. Chem. **2004**, *43*, 6366–6370

Fluorescence-Based Nitric Oxide Detection by Ruthenium Porphyrin Fluorophore Complexes

Mi Hee Lim and Stephen J. Lippard*

Department of Chemistry, Massachusetts Institute of Technology, Cambridge, Massachusetts 02139

Received December 10, 2003

The ruthenium(II) porphyrin fluorophore complexes [Ru(TPP)(CO)(Ds-R)] (TPP = tetraphenylporphinato dianion; Ds = dansyl; R = imidazole (im), **1**, or thiomorpholine (tm), **2**) were synthesized and investigated for their ability to detect nitric oxide (NO) based on fluorescence. The X-ray crystal structures of **1** and **2** were determined. The Ds-im or Ds-tm ligand coordinates to an axial site of the ruthenium(II) center through a nitrogen or sulfur atom, respectively. Both exhibit quenched fluorescence when excited at 368 or 345 nm. Displacement of the metal-coordinated fluorophore by NO restores fluorescence within minutes. These observations demonstrate fluorescence-based NO detection using ruthenium porphyrin fluorophore conjugates.

Introduction

Nitric oxide, well-known as an atmospheric pollutant, also serves as a messenger in the cardiovascular, immune, and nervous systems.[1−5] To understand these diverse biological functions, directly sensing of NO in a manner that maps its spatial and temporal distribution would be most valuable. Currently, NO can be monitored[6] by chemiluminescence,[5] amperometry,[7] EPR spectroscopy,[8−10] or fluorescence.[11−15] Research in our laboratory focuses on the synthesis of fluorescence-based sensors in which NO-induced displacement of a fluorophore, quenched when bound to a metal center, is accompanied by light emission upon excitation at a proper wavelength. Previous applications of this strategy revealed that [Co(^{R}DATI)$_2$], [Co(DATI-4)], and [Rh$_2$(μ-OAc)$_4$(Ds-R)] complexes, where DATI is dansyl aminotroponiminate and Ds-R is an imidazole or piperazine derivatized dansyl group, display dramatic increases in fluorescence upon exposure to NO.[16,17] These complexes are stable in the presence of O_2, an important requirement for biological applications, but additional tactics are required, including faster response rates and water compatibility. We have therefore been exploring other synthetic platforms to approach these goals.

Nitric oxide binds to the heme iron of soluble guanylyl cyclase (sGC) selectively over O_2.[18,19] The coordination environment of this NO-binding iron center has inspired the fabrication of fiber optic probes that are embedded with a fluorescent dye-labeled heme domain of sGC or cytochrome *c*′ to detect NO.[20,21] These probes, however, report only local

* To whom correspondence should be addressed. E-mail: lippard@mit.edu.

(1) Furchgott, R. F. *Angew. Chem., Int. Ed.* **1999**, *38*, 1870−1880.
(2) Ignarro, L. J. *Angew. Chem., Int. Ed.* **1999**, *38*, 1882−1892.
(3) Palmer, R. M. J.; Ferrige, A. G.; Moncada, S. *Nature* **1987**, *327*, 524−526.
(4) Wink, D. A.; Vodovotz, Y.; Laval, J.; Laval, F.; Dewhirst, M. W.; Mitchell, J. B. *Carcinogenesis* **1998**, *19*, 711−721.
(5) Hampl, V.; Walters, C. L.; Archer, S. L. In *Methods in Nitric Oxide Research*; Feelisch, M., Stamler, J. S., Eds.; Wiley: New York, 1996; pp 309−318.
(6) Nagano, T.; Yoshimura, T. *Chem. Rev.* **2002**, *102*, 1235−1270.
(7) Mao, L.; Tian, Y.; Shi, G.; Liu, H.; Jin, L.; Yamamoto, K.; Tao, S.; Jin, J. *Anal. Lett.* **1998**, *31*, 1991−2007.
(8) Kotake, Y.; Tanigawa, T.; Tanigawa, M.; Ueno, I.; Allen, D. R.; Lai, C.-S. *Biochim. Biophys. Acta* **1996**, *1289*, 362−368.
(9) Yoshimura, T.; Fujii, S.; Yokoyama, H.; Kamada, H. *Chem. Lett.* **1995**, 309−310.
(10) Komarov, A. M.; Lai, C.-S. *Biochim. Biophys. Acta* **1995**, *1272*, 29−36.
(11) Kojima, H.; Nakatsubo, N.; Kikuchi, K.; Kawahara, S.; Kirino, Y.; Nagoshi, H.; Hirata, Y.; Nagano, T. *Anal. Chem.* **1998**, *70*, 2446−2453.
(12) Kojima, H.; Urano, Y.; Kikuchi, K.; Higuchi, T.; Hirata, Y.; Nagano, T. *Angew. Chem., Int. Ed.* **1999**, *38*, 3209−3212.
(13) Miles, A. M.; Wink, D. A.; Cook, J. C.; Grisham, M. B. In *Methods in Enzymology*; Packer, L., Ed.; Academic Press: Boston, MA, 1996; Vol. 268, pp 105−120 and references therein.
(14) Bätz, M.; Korth, H.-G.; Sustmann, R. *Angew. Chem., Int. Ed.* **1997**, *36*, 1501−1503.
(15) Meineke, P.; Rauen, U.; de Groot, H.; Korth, H.-G.; Sustmann, R. *Chem. Eur. J.* **1999**, *5*, 1738−1747.
(16) Franz, K. J.; Singh, N.; Spingler, B.; Lippard, S. J. *Inorg. Chem.* **2000**, *39*, 4081−4092.
(17) Hilderbrand, S. A.; Lim, M. H.; Lippard, S. J. *J. Am. Chem. Soc.* **2004**, *126*, 4972−4978.
(18) Kim, S.; Deinum, G.; Gardner, M. T.; Marletta, M. A.; Babcock, G. T. *J. Am. Chem. Soc.* **1996**, *118*, 8769−8770 and references therein.
(19) Burstyn, J. N.; Yu, A. E.; Dierks, E. A.; Hawkins, B. K.; Dawson, J. H. *Biochemistry* **1995**, *34*, 5896−5903.
(20) Barker, S. L. R.; Zhao, Y.; Marletta, M. A.; Kopelman, R. *Anal. Chem.* **1999**, *71*, 2071−2075.

10.1021/ic035418n CCC: $27.50 © 2004 American Chemical Society
Published on Web 09/08/2004

NO concentrations at their tips and are unsuitable for intracellular work. An iron complex of a methoxycoumarin-pendant cyclam and 2,2,5,5-tetramethylpyrrolidine-*N*-oxide covalently linked to fluorescamine was designed as a fluorescent model of sGC. Unfortunately, this sensor is unstable in air and displays only a weak fluorescent response to NO.[22]

The reactivity of nitric oxide with metalloporphyrins has been extensively investigated.[23,24] Ruthenium porphyrins form stable nitrosyl adducts upon exposure to NO.[24−29] In the present Article, we describe the synthesis and characterization of ruthenium porphyrin complexes with axially bound fluorophores. We demonstrate that a fluorophore coordinated to ruthenium in this manner can be released by NO, resulting in turn-on fluorescence upon excitation. This ruthenium porphyrin fluorophore scaffold is, to the best of our knowledge, the first example of a fluorescent NO sensor incorporating a metalloporphyrin.

Experimental Section

General Considerations. All reagents for syntheses were purchased from Aldrich and used without further purification. Dichloromethane (CH_2Cl_2) and tetrahydrofuran (THF) were purified by passage through alumina columns under an Ar atmosphere. Diethyl ether (Et_2O), hexanes, and ethyl acetate (EtOAc) were used as received. Ds-im was synthesized as previously reported.[17] Nitric oxide (Matheson 99%) was purified as described.[17,30] NO was transferred by syringe in a glovebox. NO reactions were performed under anaerobic conditions to avoid adventitious reactions of the gas with O_2. Fluorescence emission spectra were recorded at 25.0 ± 0.2 °C on a Hitachi F-3010 spectrophotometer. NMR spectra were measured on a Varian 300 spectrometer or an Inova 500 MHz spectrometer at ambient temperature and referenced to internal ^{1}H and ^{13}C solvent peaks. FT-IR spectra were obtained on an Avatar 360 spectrophotometer and UV−vis spectra on a Hewlett-Packard 8453 diode array spectrophotometer. ESI-MS analysis was performed on an Agilent 1100 series instrument.

Dansyl-thiomorpholine (Ds-tm). To a solution of dansyl chloride (2.90 g, 10.7 mmol) in 200 mL of THF were added thiomorpholine (1.11 g, 10.7 mmol) and Cs_2CO_3 (4.18 g, 12.8 mmol). The reaction was allowed to stir overnight and filtered, and the solvent was removed by rotary evaporation. The crude solids were purified by column chromatography (silica, 6:1 hexanes/EtOAc; R_f = 0.29 by TLC), yielding a yellow product (2.82 g, 8.38 mmol, 77%): mp 144−146 °C. ^{1}H NMR (500 MHz, $CDCl_3$): δ 8.56 (1H, d, J = 5 Hz), 8.3 (1H, d, J = 10 Hz), 8.19 (1H, dd, J = 7.25, 1.5 Hz), 7.57−7.51 (2H, m), 7.19 (1H, dd, J = 7.5, 0.5 Hz), 3.55−3.53 (4H, m), 2.89 (6H, s), 2.67−2.64 (4H, m). ^{13}C NMR (125 MHz, $CDCl_3$): δ 152.0, 133.6, 130.9, 130.5, 130.3, 130.2, 128.3, 123.3, 119.5, 115.5, 47.5, 45.6, 27.5. IR (KBr; cm^{-1}): 2985 (w), 2953 (w), 2917 (w), 2862 (w), 2825 (w), 2783 (w), 1612 (w), 1590 (m), 1579 (m), 1572 (m), 1501 (w), 1478 (w), 1463 (w), 1443 (w), 1411 (m), 1401 (m), 1379 (w), 1355 (m), 1319 (m), 1288 (m), 1228 (w), 1199 (w), 1183 (w), 1171 (w), 1140 (m), 1102 (w), 1080 (m), 1043 (w), 1018 (w), 965 (m), 942 (w), 914 (s), 835 (w), 814 (w), 801 (w), 789 (m), 775 (w), 689 (s), 659 (m), 623 (m), 569 (s), 530 (w), 502 (w), 452 (m). ESI(+)MS (m/z) [M + H]$^+$ Calcd for $C_{16}H_{21}N_2O_2S_2$: 337.1. Found: 337.4.

[Ru(TPP)(CO)(Ds-im)] (1). A portion of Ds-im (55 mg, 0.18 mmol) was added to a solution of [Ru(TPP)(CO)] (45 mg, 0.060 mmol) in 2 mL of CH_2Cl_2, after which Et_2O was slowly diffused into the solution at 0 °C. Purple crystals of X-ray quality were grown over 1 day and isolated in 93% yield (0.058 g, 0.056 mmol). IR (KBr; cm^{-1}): 3164 (w), 3144 (w), 3126 (w), 3103 (w), 3074 (w), 3045 (w), 3022 (w), 2972 (w), 2945 (w), 2971 (w), 2945 (w), 2864 (w), 2830 (w), 2788 (w), 2771 (w), 1938 (s), 1593 (m), 1568 (w), 1437 (m), 1387 (m), 1350 (m), 1304 (m), 1261 (w), 1202 (w), 1176 (m), 1163 (m), 1062 (m), 1008 (s), 934 (w), 834 (w), 796 (m), 757 (m), 751 (m), 736 (w), 717 (m), 700 (m), 677 (w), 664 (w), 636 (m), 591 (m), 559 (w), 538 (w), 525 (w), 492 (w), 461 (w). UV−vis in CH_2Cl_2 [λ_{max}/nm (ϵ, M^{-1} cm^{-1})]: 313 (2.0×10^4), 413 (2.3×10^5), 534 (2.0×10^4), 567 (4.6×10^3), 601 (1.3×10^3). ^{1}H NMR (300 MHz, CD_2Cl_2): δ 8.60 (8H, s), 8.43 (1H, d, J = 8.5 Hz), 8.26−8.22 (4H, m), 7.90 (4H, dm, J = 7.3 Hz), 7.78−7.64 (14H, m), 7.52 (1H, dd, J = 7.6, 1.1 Hz), 7.32−7.19 (3H, m), 7.13 (1H, d, J = 7.7 Hz), 6.46 (1H, d, J = 8.8 Hz), 2.83 (6H, s). ^{13}C NMR (100 MHz, $CDCl_3$): δ 180.1, 152.3, 143.3, 142.4, 134.0, 133.8, 133.1, 131.4, 131.2, 130.0, 129.9, 129.1, 128.1, 127.0, 126.3, 126.0, 123.4, 122.4, 121.2, 115.5, 115.3, 114.3, 45.1. Anal. Calcd for $C_{60}H_{43}N_7O_3RuS$: C, 69.08; H, 4.15; N, 9.40. Found: C, 68.78; H, 4.21; N, 9.09.

[Ru(TPP)(CO)(Ds-tm)] (2). A portion of Ds-tm (9.1 mg, 0.027 mmol) was added to a solution of [Ru(TPP)(CO)] (10 mg, 0.013 mmol) in 2 mL of CH_2Cl_2. The resulting solution was layered with hexanes and cooled to 0 °C. Purple crystals of X-ray quality were grown over 4 days and collected (0.013 g, 0.012 mmol, 91%). UV−vis in CH_2Cl_2 [λ_{max}/nm (ϵ, M^{-1} cm^{-1})]: 312 (2.5×10^4), 412 (2.1×10^5), 531 (2.1×10^4), 569 (5.1×10^3), 602 (2.0×10^3). IR (KBr; cm^{-1}): 3104 (w), 3075 (w), 3052 (w), 3022 (w), 2985 (w), 2943 (w), 2937 (w), 2865 (w), 2832 (w), 2790 (w), 1951 (s), 1595 (m), 1574 (w), 1568 (w), 1527 (m), 1503 (w), 1486 (w), 1477 (w), 1453 (w), 1440 (m), 1405 (w), 1394 (w), 1373 (w), 1350 (m), 1320 (w), 1305 (m), 1282 (w), 1264 (w), 1230 (w), 1216 (w), 1201 (w), 1175 (m), 1157 (w), 1141 (m), 1094 (w), 1071 (s), 1008 (s), 962 (w), 945 (w), 909 (m), 885 (m), 846 (w), 834 (w), 793 (s), 754 (m), 737 (m), 716 (m), 700 (s), 672 (w), 664 (w), 637 (w), 619 (w), 595 (w), 577 (w), 567 (m), 540 (w), 527 (w), 499 (w), 462 (w),452 (w), 415 (w). ^{1}H NMR (500 MHz, CD_2Cl_2): δ 8.64 (8H, s), 8.51 (1H, s), 8.22 (4H, br, s), 8.00 (4H, br, s), 7.76−7.64 (14H, m), 7.36 (2H, s), 7.16 (1H, s), 2.86 (6H, s), 1.11 (4H, br, s), −2.23 (4H, br, s). Anal. Calcd for $C_{61}H_{48}N_6O_3RuS_2\cdot CH_2Cl_2$: C, 64.02; H, 4.33; N, 7.22. Found: C, 64.47; H, 4.29; N, 7.21.

X-ray Crystallographic Studies. A suitable crystal was mounted in Paratone N oil on the tip of a glass capillary and frozen under a −100 °C nitrogen cold stream. Data were collected on a Bruker APEX CCD X-ray diffractometer with Mo Kα radiation (λ = 0.71073 Å) controlled by the SMART software package and refined and solved with the SAINTPLUS and SHELXTL software

(21) Barker, S. L. R.; Clark, H. A.; Swallen, S. F.; Kopelman, R.; Tsang, A. W.; Swanson, J. A. *Anal. Chem.* **1999**, *71*, 1767−1772.
(22) Soh, N.; Imato, T.; Kawamura, K.; Maeda, M.; Katayama, Y. *Chem. Commun.* **2002**, 2650−2651.
(23) Hoshino, M.; Laverman, L.; Ford, P. C. *Coord. Chem. Rev.* **1999**, *187*, 75−102 and references therein.
(24) Ford, P. C.; Lorković, I. M. *Chem. Rev.* **2002**, *102*, 993−1017.
(25) Miranda, K. M.; Bu, X.; Lorković, I.; Ford, P. C. *Inorg. Chem.* **1997**, *36*, 4838−4848.
(26) Lorković, I. M.; Miranda, K. M.; Lee, B.; Bernhard, S.; Schoonover, J. R.; Ford, P. C. *J. Am. Chem. Soc.* **1998**, *120*, 11674−11683.
(27) Lorković, I. M.; Ford, P. C. *Inorg. Chem.* **1999**, *38*, 1467−1473.
(28) Lorković, I. M.; Ford, P. C. *Chem. Commun.* **1999**, 1225−1226.
(29) Kadish, K. M.; Adamian, V. A.; Van Caemelbecke, E.; Tan, Z.; Tagliatesta, P.; Bianco, P.; Boschi, T.; Yi, G.-B.; Khan, M. A.; Richter-Addo, G. B. *Inorg. Chem.* **1996**, *35*, 1343−1348.
(30) Lorković, I. M.; Ford, P. C. *Inorg. Chem.* **2000**, *39*, 632−633.

packages.[31−33] The general procedures used for data collection are reported elsewhere.[34] Empirical absorption corrections were calculated with the SADABS program.[35] The structures of **1** and **2** were solved by standard Patterson and difference Fourier methods. All non-hydrogen atoms were refined anisotropically, and the structure solution was checked for higher symmetry with PLATON.[36] In the crystal structure of **1**, a disordered Et_2O molecule in the lattice was refined over two positions, each with a 0.5 occupancy factor. One and one-half CH_2Cl_2 molecules in the structure of **2** were disordered. In the first disordered CH_2Cl_2, one of the chlorine atoms resides in two positions with occupancy factors of 0.6 and 0.4. In the remaining 0.5 CH_2Cl_2, the carbon atom was disordered over two sites modeled with occupancy factors of 0.6 and 0.4. The highest electron density in the final difference Fourier maps for **1** and **2** was 1.57 and 1.40 e/Å^3, respectively, in the vicinity of the ruthenium atom.

Results and Discussion

Syntheses of Fluorophore-Derived Ruthenium Porphyrin Complexes. Ruthenium carbonyl tetraphenylporphyrin complexes [Ru(TPP)(CO)(L)], with L = Ds-im (**1**) or Ds-tm (**2**), were readily prepared from solutions of [Ru(TPP)(CO)] and the dansyl-derivatized axial base, imidazole or thiomorpholine, in CH_2Cl_2. Crystals of **1** were grown by vapor diffusion of Et_2O into the resulting solution over 1 day at 0 °C and isolated in 93% yield. When a CH_2Cl_2 solution of [Ru(TPP)(CO)] and Ds-tm was layered with hexanes, X-ray quality crystals of **2** were grown over 4 days at 0 °C in 91% yield.

X-ray Crystal Structure Determinations of [Ru(TPP)(CO)(Ds-im)] (1) and [Ru(TPP)(CO)(Ds-tm)] (2). Crystallographic data for **1** and **2** are summarized in Table 1, and selected bond distances and angles are contained in Table 2. The crystal structures of **1** and **2** indicate that the fluorophores are coordinated to the axial site of the ruthenium center trans to the carbonyl group via the nitrogen atom of imidazole and the sulfur atom of thiomorpholine, respectively (Figure 1). In the crystal structure of **1**, the Ru−C_{CO} and Ru−N_{im} distances, 1.834(4) Å and 2.166(3) Å, and the Ru−C−O and N_{im}−Ru−C_{CO} angles, 179.3(3)° and 179.58(15)°, are consistent with those in the [Ru(TPP)(CO)(1-MeIm)] analogue reported previously.[37,38] Compound **2** is the first crystallographically characterized ruthenium porphyrin complex that contains sulfur-donor axial ligand trans to a carbonyl group. The Ru−S bond length, 2.500(2) Å, is the longest reported for ruthenium porphyrin complexes containing S-donor axial ligands,[39,40] reflecting the strong trans influence of the carbonyl ligand.

Table 1. Summary of X-ray Crystallographic Data

	[Ru(TPP)(CO)(Ds-im)]·0.5Et_2O (**1**)	[Ru(TPP)(CO)(Ds-tm)]·1.5CH_2Cl_2 (**2**)
formula	$C_{62}H_{48}N_7O_{3.5}RuS$	$C_{62.5}H_{51}Cl_3N_6O_3RuS_2$
fw	1080.20	1205.63
space group	$P2_1/c$	$P\bar{1}$
a, Å	12.773(3)	11.241(2)
b, Å	20.264(4)	15.233(3)
c, Å	20.711(4)	16.615(3)
α, deg		97.00(3)
β, deg	107.79(3)	97.90(3)
γ, deg		103.00(3)
V, Å^3	5104.3(18)	2711.2(9)
Z	4	2
ρ_{calc}, g/cm^3	1.406	1.477
T, °C	−100	−100
μ(Mo Kα), mm^{-1}	0.405	0.568
total no. of data	37390	19865
no. of unique data	9023	9094
no. of params	694	770
R^a	0.0514	0.0744
$wR2^b$	0.1224	0.1489
max, min peaks, e/Å^3	1.570, −0.557	1.403, −0.716

^{a} $R = \sum||F_o| - |F_c||/\sum|F_o|$. ^{b} $wR^2 = \{w(F_o^2 - F_c^2)^2/\sum[w(F_o^2)^2]\}^{1/2}$.

Table 2. Selected Bond Distances (Å) and Angles (deg)[a]

	[Ru(TPP)(CO)(Ds-im)] (**1**)		
Ru1−N1	2.056(3)	Ru1−C45	1.834(4)
Ru1−N2	2.049(3)	C45−O1	1.139(5)
Ru1−N3	2.045(3)	C45−Ru1−N5	179.58(15)
Ru1−N4	2.055(3)	O1−C45−Ru1	179.3(3)
Ru1−N5	2.166(3)		
	[Ru(TPP)(CO)(Ds-tm)] (**2**)		
Ru1−N1	2.045(5)	Ru1−C45	1.817(8)
Ru1−N2	2.051(5)	C45−O1	1.140(8)
Ru1−N3	2.040(6)	C45−Ru1−S1	173.2(2)
Ru1−N4	2.054(5)	O1−C45−Ru1	177.4(7)
Ru1−S1	2.500(2)		

[a] Numbers in parentheses are estimated standard deviations of the last significant figures. Atoms are labeled as indicated in Figure 1.

Fluorescence Properties. Fluorescence studies revealed 39-fold and 2.0-fold quenching of the dansyl group fluorescence in **1** and **2**, respectively, when compared to that of the free Ds-im or Ds-tm ligands (Figures 2 and S1). In the solid state, **1** and **2** are not fluorescent. Upon addition of NO to solutions of these compounds, an increase in fluorescence was observed. Reaction of a 10 μM dichloromethane solution of **1** with 100 equiv of NO afforded a 19-fold increase in the integrated fluorescence emission (Figure 3). The fluorescence response was complete in less than 20 min. Restoration of fluorescence to the value of free Ds-im in the reaction of **1** with NO does not occur, most likely due to an inner filter effect. Ruthenium porphyrin complexes have strong absorbance bands at the wavelengths where excitation and emission of the fluorophore occurs, thus absorbing some of the light excitation and emission, resulting in a diminished fluorescence response. A similar effect was observed in the reaction of **2** with NO. When 100 equiv of

(31) *SMART: Software for the CCD Detector System*, version 5.626; Bruker AXS: Madison, WI, 2000.
(32) *SAINTPLUS: Software for the CCD Detector System*, version 5.01; Bruker AXS: Madison, WI, 1998.
(33) *SHELXTL: Program Library for Structure Solution and Molecular Graphics*, version 6.2; Bruker AXS: Madison, WI, 2000.
(34) Kuzelka, J.; Mukhopadhyay, S.; Spingler, B.; Lippard, S. J. *Inorg. Chem.* **2004**, *43*, 1751−1761.
(35) Sheldrick, G. M. *SADABS: Area-Detector Absorption Correction*; University of Göttingen: Göttingen, Germany, 2001.
(36) Spek, A. L. *PLATON, A Multipurpose Crystallographic Tool*; Utrecht University: Utrecht, The Netherlands, 2000.
(37) Slebodnick, C.; Seok, W. K.; Kim, K.; Ibers, J. A. *Inorg. Chim. Acta* **1996**, *243*, 57−65.
(38) Salzmann, R.; Ziegler, C. J.; Godbout, N.; McMahon, M. T.; Suslick, K. S.; Oldfield, E. *J. Am. Chem. Soc.* **1998**, *120*, 11323−11334.
(39) James, B. R.; Pacheco, A.; Rettig, S. J.; Ibers, J. A. *Inorg. Chem.* **1988**, *27*, 2414−2421.
(40) Yi, G.-B.; Khan, M. A.; Richter-Addo, G. B. *Chem. Commun.* **1996**, 2045−2046.

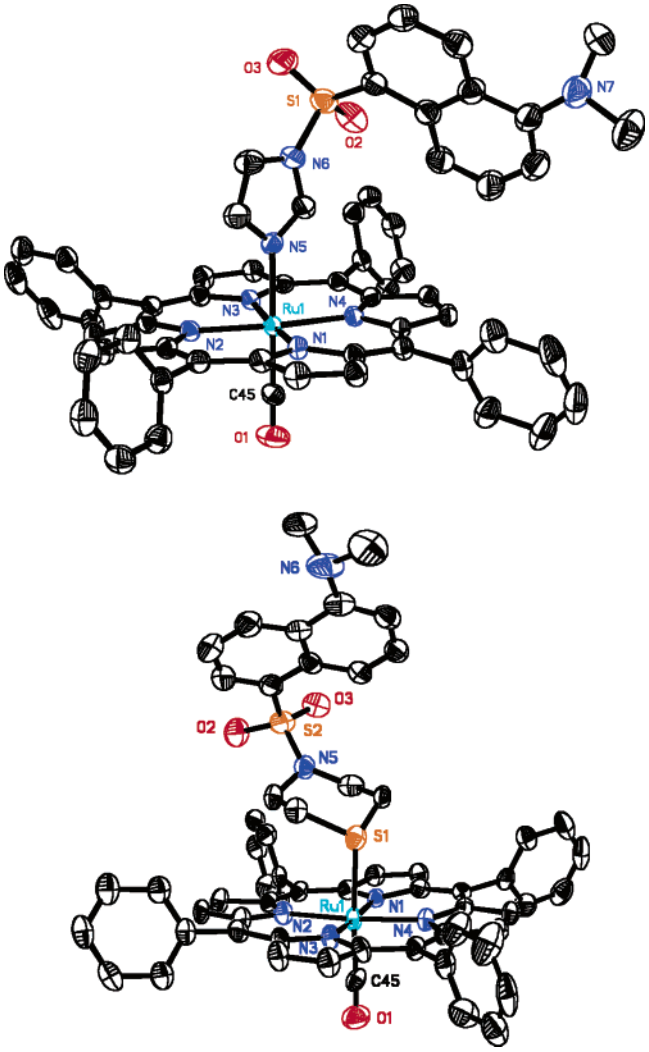

Figure 1. ORTEP diagrams of [Ru(TPP)(CO)(Ds-im)] (top) and [Ru(TPP)-(CO)(Ds-tm)] (bottom) showing 50% thermal ellipsoids.

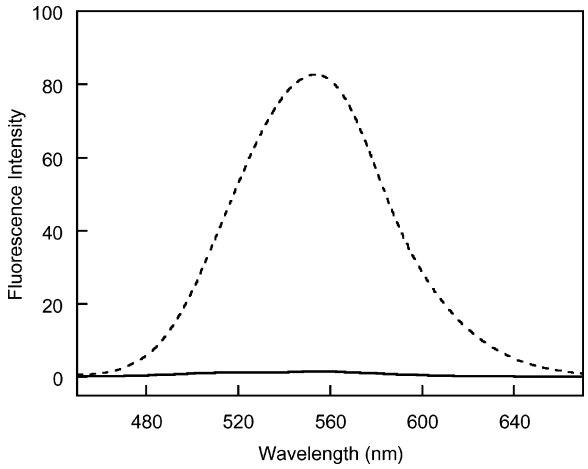

Figure 2. Fluorescence emission spectra of [Ru(TPP)(CO)(Ds-im)] (—) and Ds-im (- - -) in CH_2Cl_2.

NO was introduced into a 10 μM dichloromethane solution of **2**, a 1.3-fold increase in fluorescence was exhibited (Figure S2). The response is much more rapid, however, being complete in 3 min. Compounds **1** and **2** display turn-on fluorescent detection of NO that is 1−2 orders of magnitude more rapid than our previously reported Co(II) sensors.[16]

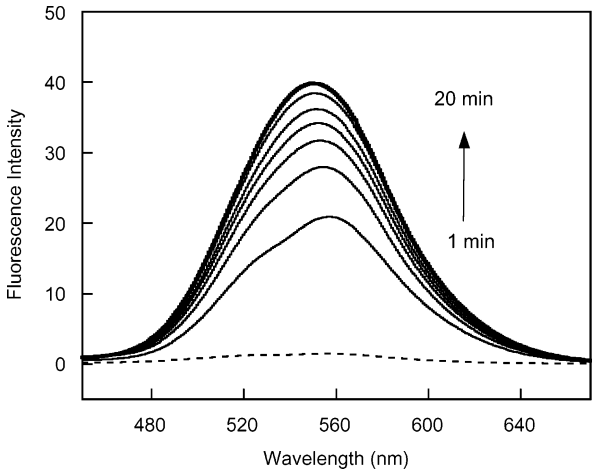

Figure 3. Fluorescence response of 10 μM [Ru(TPP)(CO)(Ds-im)] in CH_2Cl_2 upon addition of 100 equiv of NO (—). Individual spectra were recorded at 1, 3, 5, 10, 15, and 20 min. Dashed line is at 0 min.

Scheme 1

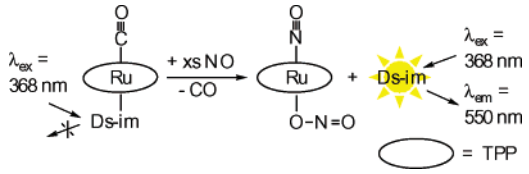

Nature of the Reaction of [Ru(TPP)(CO)(Ds-im)] (1) with Nitric Oxide. When [Ru(TPP)(CO)] is treated with excess NO, the product is [Ru(TPP)(NO)(ONO)].[25,29] In order to determine whether similar chemistry might apply in the present case, the Ru-containing product from the reaction of **1** with NO was isolated from a CH_2Cl_2/pentane solution under anaerobic conditions and characterized by IR and UV−vis spectroscopy. The data were consistent with those previously reported for [Ru(TPP)(NO)(ONO)].[25,29] An X-ray analysis of crystals grown by the slow evaporation of a CH_2Cl_2 solution of the complex isolated from the NO reaction revealed the presence of [Ru(TPP)(NO)(ONO)] (57% yield), with an 8-fold disorder in the axial ligands. The X-ray crystal structure is consistent with those previously reported in the literature.[25] In addition, the ^{1}H NMR spectrum of the reaction of **1** with NO indicated the presence of free Ds-im. Taken together, these results demonstrate that nitric oxide treatment causes both Ds-im and CO to dissociate from the axial sites of the Ru(II) center (Scheme 1). We therefore conclude that the fluorescence enhancement of **1** and **2** observed upon reaction with NO arises from displacement of Ds-im or Ds-tm from their axial positions, liberating the fluorophores from the quenching environment of the Ru(II) center and restoring fluorescence.

Conclusions

New fluorophore-derived ruthenium porphyrin complexes have been prepared, which can be used for direct fluorescence-based detection of NO. The fluorescence increase observed during the reaction of these nonfluorescent complexes with NO is the result of the dissociation of fluorophore from the axial site of the ruthenium center. This study further demonstrates the value of fluorophore displacement as a valid

strategy for the development of NO sensors and paves the way for the development of water-soluble, even more rapidly responding metalloporphyrins toward the ultimate goal of sensing nitric oxide in living cells.

Acknowledgment. This work was supported by NSF Grant CHE-0234951. We thank Dr. Sumitra Mukhopadhyay and Dr. Peter Mueller for assistance with the X-ray structure determinations and Dr. Scott A. Hilderbrand for helpful discussions. The MIT DCIF NMR spectrometer was funded through NSF Grants CHE-9808061 and DBI-9729592.

Supporting Information Available: Figure S1 and S2 for the fluorescence studies of **2** with and without NO, and X-ray crystallographic files (CIF). This material is available free of charge via the Internet at http://pubs.acs.org.

IC035418N